Squeezed States in a Bose-Einstein Condensate

C. Orzel, A. K. Tuchman, M. L. Fenselau, M. Yasuda,* M. A. Kasevich

We report manipulation of the atom number statistics associated with Bose-Einstein condensed atoms confined in an array of weakly linked mesoscopic traps. We used the interference of atoms released from the traps as a sensitive probe of these statistics. By controlling relative strengths of the tunneling rate between traps and atom-atom interactions within each trap, we observed trap states characterized by sub-Poissonian number fluctuations and adiabatic transitions between these number-squeezed states and coherent states of the atom field. The quantum states produced in this work may enable substantial gains in sensitivity for atom interference–based instruments as well as fundamental studies of quantum phase transitions.

The study of squeezed states of the electromagnetic field (*1*), states that have sub-Poissonian fluctuations in either the number of photons or the phase of the field, is a dynamic field of quantum optics, touching on both fundamental questions of quantum measurement and practical issues in precision measurement. The use of squeezed states in optical interferometry can potentially lead to a marked improvement in interferometric measurements by allowing for statistical sensitivities that scale inversely with the number of detected photons (the Heisenberg limit) (*2*). This is of great interest in making detectors for rotation, acceleration, and even gravitational waves. The sensitivity of classical methods is limited by photon shot noise and scales inversely with the square root of the number of detected photons.

In recent years, interferometric measurement techniques have been extended to include interference of atomic de Broglie waves (*3*). The accuracy and sensitivity of atom-interferometer–based gyroscopes, gravimeters, and gravity gradiometers are comparable to the state-of-the-art detectors that use more traditional techniques.

It is natural to ask whether it is possible to combine these two techniques to further improve interferometric measurements: Is it possible to create a source of squeezed states of the atom field suitable for atom interferometry below the atom shot-noise limit? Here, we report the observation of an array of atom-number–squeezed states in an optical lattice potential populated by atoms from a Bose-Einstein condensate (BEC). This represents a step toward the goal of Heisenberg-limited atom interferometry (*4*). These states are related to spin-squeezed states that have been recently observed in nondegenerate atomic ensembles (*5–7*) and that may also be used for interferometry below the shot-noise limit (*8*, *9*).

The essential physics underlying the formation of atom-number–squeezed states in a lattice potential is illustrated by considering the many-atom ground state of a BEC in a double-well potential (*10–12*). In this model system, N bosonic atoms are confined by an infinite harmonic potential that is divided into two wells (left and right) by a barrier that can be raised and lowered arbitrarily. Making a simple two-mode approximation, considering only the lowest energy states, the creation and annihilation operators ($a^\dagger_{\mathrm{L,R}}$ and $a_{\mathrm{L,R}}$, respectively) for atoms localized in the ground state of either the left or the right potential well can be constructed. Neglecting terms that depend only on the total conserved particle number, the Hamiltonian for the system can be written

$$H = \gamma(a^\dagger_{\mathrm{L}}a_{\mathrm{R}} + a^\dagger_{\mathrm{R}}a_{\mathrm{L}}) + g\beta/2[(a^\dagger_{\mathrm{L}}a_{\mathrm{L}})^2 + (a^\dagger_{\mathrm{R}}a_{\mathrm{R}})^2] \qquad (1)$$

where $g = 4\pi a_{\mathrm{sc}}\hbar^2/m$ is the mean-field energy constant [a_{sc} is the s-wave scattering length that parameterizes the repulsive collisional interaction between condensate atoms ($a_{\mathrm{sc}} \simeq 5.8$ nm for the ^{87}Rb $F = 2$, $m_f = 2$ state), $2\pi\hbar$ is Planck's constant, and m is the atomic mass]. The term in γ describes tunneling between wells (atoms are created in one well and annihilated in the other), whereas the term in $g\beta$, which depends on the number of atoms within each well, describes the mean field energy due to interactions between atoms in the same well. The coefficients γ and β are determined from integrals over single-particle wave functions (*13*).

The ratio $Ng\beta/\gamma$ of the mean field energy per particle to the tunneling energy determines the nature of the many-body ground state. In the weak interaction, strong tunneling limit ($Ng\beta/\gamma \ll 1$), the interaction term is negligible. In this case, each atom is in a coherent superposition of left-well and right-well states, and the ground state of the system is a state with a mean number $N/2$ of atoms in each well with Poissonian fluctuations $\sigma_n \sim \sqrt{N/2}$ about that mean ($\sigma_n^2 \equiv \langle \hat{n}^2 \rangle - \langle \hat{n} \rangle^2$, with $\hat{n}$ the number operator for the left or right well). The states in each well are quasi-coherent states as the total number of atoms in the system is fixed (*14*). Because the difference between these states and full coherent states becomes small for large N, we refer to these states simply as coherent states. In the opposite limit of strong interactions or weak tunneling ($Ng\beta/\gamma \gg 1$), the tunneling term is negligible. In this case, the Hamiltonian is the product of number operators for the left and right wells, and the eigenstates are products of Fock states ($\sigma_n = 0$) (*15*). For arbitrary $Ng\beta/\gamma$, σ_n decreases monotonically as we increase the interactions between atoms or decrease the rate of tunneling, scaling as $(Ng\beta/\gamma)^{-1/4}$ for $Ng\beta/\gamma \gtrsim 1$ until $Ng\beta/\gamma \simeq N^2$ (corresponding to $\sigma_n \simeq 1/2$). At values of $Ng\beta/\gamma \simeq N^2$, the system rapidly localizes to Fock states (*11*). This regime is analogous to the insulating phase of the Mott insulator transition in a lattice system (*16*). We note that the Gross-Pitaevskii equation, which assumes that the many-atom wave function can be factorized into the product of identical single-atom wave functions, cannot be used to model the formation of squeezed states.

Our experimental realization of number-squeezed states is not in a two-well potential but in a one-dimensional array of wells with ~12 wells populated. The array is formed by loading a BEC into an optical lattice potential, which is generated by a standing wave laser field. We do not control the total number of atoms loaded into the lattice. We change the ratio $Ng\beta/\gamma$ by varying the intensity of the lattice laser and the initial condensate density. In this way, we create an array of number-squeezed states in the populated lattice sites. We observe the formation of squeezed states by exploiting the phase-sensitive interference of atoms released from the lattice (*17*, *18*) to detect the increase in phase variance σ_ϕ associated with the reduced number variance σ_n at each lattice site ($\sigma_\phi \propto 1/\sigma_n$).

The theoretical problem is generalized to the case of multiple wells by considering a sinusoidally varying external potential with depth U_0 superimposed on the weaker harmonic confining potential that initially supports the BEC. Invoking the assumptions introduced above for the two-well problem results in the well-known Bose-Hubbard Hamiltonian (*16*, *19–21*). We solve for the ground state of this system variationally using trial wave functions that characterize the state at the ith lattice site by a Gaussian number distribution of mean number N_i and variance σ_{ni}. Our numerical estimates of the variational parameters N_i and σ_{ni} are in excellent

Physics Department, Yale University, New Haven, CT 06520, USA.

*Permanent address: University of Tokyo 2-11-16 Yayoi Bunkyo-Ku Tokyo, 113-8656, Japan.

agreement with reported analytic results (20) (obtained for a uniform lattice in the limit $\sigma_{ni} > 1/2$). In particular, $\sigma_{ni} \propto (N_i g\beta/\gamma)^{-1/4}$ for $N_i g\beta/\gamma \gtrsim 1$. When $\sigma_{ni} \lesssim 1/2$, the system undergoes a quantum (Mott insulator) phase transition to a state with a Fock state in each well. In the experimental work described below, we investigate the regime $\sqrt{N_i} \gtrsim \sigma_{ni} \gtrsim 1/2$. Finally, we note that a few-well system is mathematically analogous to recently studied spinor condensate systems (22, 23).

The apparatus used to create our BEC has been described in detail (24). We load $\sim 10^8$ ^{87}Rb atoms into a time-orbiting potential (TOP) trap and evaporatively cool the sample through a combination of TOP and forced radio frequency evaporation. We produce pure condensates of $F = 2$, $m_f = 2$ atoms that contain $\sim 10^4$ atoms at nearly zero temperature. After the evaporation cycle is complete, we adiabatically relax the trapping potential by reducing the quadrupole component of the TOP field, thereby increasing the size and decreasing the density of our sample. For typical final trap parameters, we have a radial trap oscillation frequency of $\omega_\perp \sim 2\pi \times 19$ s^{-1}, with 3×10^4 condensate atoms at a density of 5×10^{13} cm^{-3}.

After the adiabatic relaxation, we apply a vertically oriented one-dimensional optical lattice to the sample by illuminating the sample with laser light at $\lambda = 840$ nm. The light is focused to a $1/e$ intensity radius of 50 μm and retroreflected to form a standing wave. This produces a sinusoidally varying ac Stark shift of the atomic ground state. The large detuning of this laser from the ^{87}Rb resonance at 780 nm allows us to obtain substantial light shifts with negligible spontaneous emission, creating a periodic array of potential wells at the antinodes of the light field, with well depths up to $\sim 50\ E_R$ (where $E_R \equiv \hbar^2 k^2/2m$ is the recoil energy from absorption of a 840-nm photon and $k = 2\pi/\lambda$). The lattice light field also provides strong transverse confinement in addition to providing periodic confinement along the propagation axis. At a 50 E_R depth, the transverse oscillation frequency is $2\pi \times 120$ s^{-1}, substantially larger than the frequency associated with confinement in the magnetic trap alone.

We load the lattice by linearly increasing the intensity of the lattice laser, reaching a well depth U_0 in a loading time τ_r between 2 and 200 ms. For $\tau_r = 200$ ms, the intensity ramp is approximately adiabatic, and the lattice system remains in its many-body ground state throughout the ramp. In particular, this ramp time is slow enough that excitation of phononlike longitudinal modes (20) and collective modes in individual wells (25, 26) is negligible. On the other hand, for $\tau_r = 2$ ms, the intensity ramp is nonadiabatic and excites higher lying energy states. Both limits, as well as the boundary between these extremes, are investigated below.

We probe the phase state of the system by switching off both the quadrupole component of the TOP field (27) and the lattice trapping potential, releasing the atoms to fall under the influence of gravity. As the sample falls, the clouds of atoms released from each lattice site expand ballistically so that they overlap and interfere with atoms released from neighboring sites (18). The contrast of the resulting interference pattern is used as a phase probe to distinguish between the limits of coherent and Fock states.

For a sample in which the wave function at each lattice site is a coherent state, the density distribution in the vertical direction at a time t after release from the lattice consists of peaks spaced by $2v_R t$ (where $v_R = 5.4$ mm/s is the photon recoil velocity), with an overall intensity envelope determined by the localization of the atoms within the lattice sites. For our experimental parameters, the localization is such that we observe at most two peaks in the interference signal. We hold the atoms in the lattice potential for a short time (2.5 ms) after switching off the TOP quadrupole field. This allows the gravitational potential difference between wells to establish a relative phase difference between wells (28) that shifts the interference pattern to produce a signal with two equally populated peaks (18).

For a lattice having a Fock state at each site, the interference peaks are unresolved. Although the interference of two Fock states produces an interference pattern indistinguishable from that of two coherent states with a random relative phase (29, 30), the observation of interference from atoms released from the ~ 12 sites in our lattice may be viewed as a measurement that projects a random phase onto each site: The interference of 12 sources with random phases does not show well-resolved fringes. For states with larger phase variance than a coherent state, either due to number squeezing or some other dephasing mechanism, the interference contrast decreases with increasing variance.

We take absorption images of the atomic density distribution after 8 ms of expansion, obtaining pictures like those in Fig. 1 for a lattice loaded with $\tau_r = 200$ ms. The atoms are released from the lattice after the lattice depth reaches its maximum. For low lattice depths, and thus low $Ng\beta/\gamma$ (here and below N refers to the number of atoms in the central well), we see two well-resolved peaks in the interference signal. At larger well depths, the contrast between peaks is lost, indicating an increased phase variance. Vertical cross sections through the atomic density distributions are shown in Fig. 1, D to F. The solid lines represent fits to the data of two Gaussians constrained to have the same $1/e$ width, with the heights of the individual peaks and the separation between them allowed to vary. We characterize the contrast by the ratio ζ of the width of a single peak to the separation between the peaks. For $\zeta \sim 0.5$, the distribution looks like a single broad peak.

We extract the phase variance σ_ϕ from ζ by comparing measured cross sections with a numerical model of the interference signal. The model is based on the interference of expanding Gaussian wave packets, each assigned a random phase from a distribution with a prescribed variance determined by the degree of number squeezing, as described below. Figure 2 shows the squeezing factor S defined by $\sigma_\phi^2 = S\sigma_{\phi 0}^2$ as a function of $Ng\beta/\gamma$, where $\sigma_{\phi 0}$ is the phase variance for $Ng\beta/\gamma \ll 1$. We estimate the mean-field energy $Ng\beta$ from the inferred size of our condensate (31) and the measured number of atoms and estimate the tunneling energy γ from a calculation of the band structure in the tight binding limit. The observed squeezing factor increases to a maximum of ~ 16 dB. The solid line shows the predicted dependence of $S = (Ng\beta/\gamma)^{1/2}$ (valid for $Ng\beta/\gamma \gtrsim 1$). A fit to the data of $(Ng\beta/\gamma)^c$ for $\omega_\perp = 2\pi \times 19$ s^{-1} and $Ng\beta/\gamma < 10^3$ gives $c = 0.54 \pm 0.09$. The apparent saturation at larger $Ng\beta/\gamma$ is an artifact of the analysis method, which be-

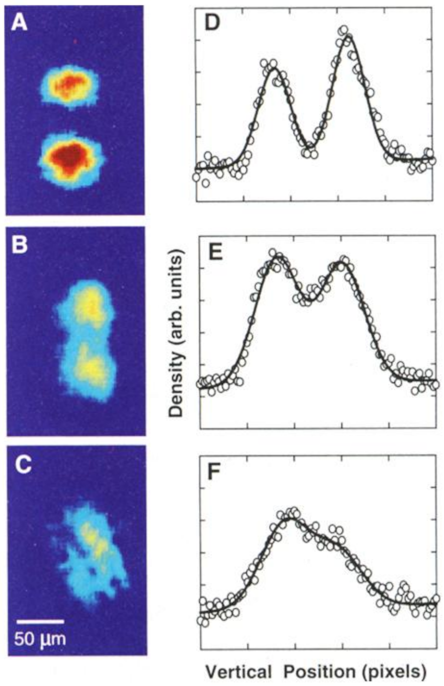

Fig. 1. Absorption images (**A** to **C**) and the associated density cross sections (**D** to **F**) of atoms released from the lattice. The two-peaked structure is due to interference between atoms released from different lattice sites. Lattice well depths: (A) $U_0 = 7.2\ E_R$, (B) $U_0 = 18\ E_R$, and (C) $U_0 = 44\ E_R$. These well depths correspond to values of $Ng\beta/\delta = 3$, 10^2, and 10^5 and observed values of $\zeta = 0.22$, 0.34, and 0.46, respectively.

comes less reliable as ζ approaches 0.5 (where the interference signal appears as a single broad peak). At values of $Ng\beta/\gamma = 10^5$, the inferred squeezing factor is 25 dB, corresponding to a phase variance of 0.5 rad and number variance $\sigma_n \simeq 1$ atom in the central well. The largest experimentally obtained value of $Ng\beta/\gamma$ is an order of magnitude away from the Mott insulator transition point, which is expected at $Ng\beta/\gamma \sim 10^6$ for our parameters (*16*). However, at $Ng\beta/\gamma = 10^5$, wells with less than 125 atoms (about 10% of the wells) are above the predicted transition point. We see no fundamental barriers to bringing the entire lattice through the transition in future work. This may provide access to a source of number-squeezed states of unprecedented purity.

The phase sensitivity of the interference signal also allows investigation of other dephasing mechanisms. Figure 3 shows a measurement of inhomogeneous phase broadening (phase dispersion). This measurement was made by raising the well depth to $U_0 \sim 30\ E_R$ in a time scale that is long compared with the time scale for oscillations within one potential well, but shorter than the time scale for adiabaticity with respect to the many-body ground state. The atoms remain in the lowest vibrational state of each potential well, but not in the full many-body ground state of the system. In this case, we effectively break the condensate up into ~12 subcondensates, whose mean phases evolve independently. After loading the lattice in this way, we hold the atoms in the combined TOP and lattice potential for a time t_{hold} before releasing them and observing the interference peaks. Figure 3 shows ζ as a function of t_{hold} for a sample with $\omega_\perp = 2\pi \times 19\ \mathrm{s}^{-1}$. For short hold times, the interference peaks are well resolved ($\zeta \sim 0.22$), as the mean phases have not had time to evolve. For longer hold times, ζ increases as the mean phases of the condensates in each well evolve independently at different rates because of differences in chemical potential between wells (*32*). Fitting sigmoidal curves to the data (solid line) for several values of $\omega_\perp$ to extract a dephasing time τ_d, we find that τ_d is inversely proportional to the curvature of the external TOP harmonic potential (inset to Fig. 3). Here the chemical potential inhomogeneity arises from an imbalance between the mean field energy and the external potential at each lattice site and is proportional to the curvature of the external potential.

The dotted line in Fig. 3 shows ζ versus t_{hold} for a lattice with $U_0 = 18\ E_R$ and $\tau_r = 200$ ms. We see that $\zeta = 0.32$ at $t = 0$ and find no substantial change in contrast for hold times up to 150 ms. Here the atoms are in the many-body ground state at $t_{\mathrm{hold}} = 0$, which shows larger phase variance than the corresponding $\tau_r = 2$ ms data because of number squeezing. As the ground state is a stationary state, the phase variance does not evolve in time.

As the squeezing occurs in the ground state of the system, the model also predicts the possibility of adiabatic transitions from squeezed to coherent states. For example, the system should move adiabatically from an initial coherent state into a squeezed state and then back to a coherent state when U_0 is first increased and then decreased (Fig. 4A). For this experiment, we load the lattice with $\tau_r = 200$ ms to a well depth $U_0^{(\mathrm{max})} \sim 40\ E_R$ (where we observe a large phase variance) and then reduce the well depth at the same rate to a level $U_0^{(\mathrm{release})} \sim 10\ E_R$ (where we observe well-resolved interference peaks). Figure 4B shows the interference signal for atoms released directly from a lattice at $U_0^{(\mathrm{release})}$ after a $\tau_r = 200$ ms ramp. Figure 4C shows atoms released directly from a lattice at $U_0^{(\mathrm{max})}$, again after a $\tau_r = 200$ ms ramp. Figure 4D shows the interference signal after the lattice is raised to $U_0^{(\mathrm{max})}$ in $\tau_r = 200$ ms and then lowered to $U_0^{(\mathrm{release})}$ in 150 ms. The interference peaks in this case are less well-resolved than those at the low lattice depth, but the contrast is markedly better than that at the high lattice depth. Figure 4, F to H, shows the result of a similar experiment carried out with $\tau_r = 2$ ms, shown schematically in Fig. 4E. The lattice potential is raised to $U_0^{(\mathrm{max})}$ quickly, maintained at that level for 10 ms, long enough for the dephasing seen in Fig. 3 to take place, and then decreased over ~ 150 ms to $U_0^{(\mathrm{release})}$. This decrease is at the same rate as in Fig.

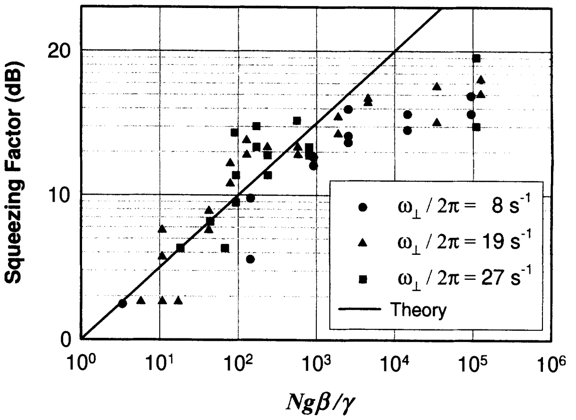

Fig. 2. Squeezing factor S as a function of the control parameter $Ng\beta/\gamma$ (evaluated for the center lattice site), for three different initial condensate densities. We varied the initial condensate density by varying the strength of the harmonic TOP trap. We extract the squeezing factor from our data by comparing observed values of ζ with those obtained from simulated data sets. We simulate our interference signals with a simple one-dimensional model. This model evaluates the interference of an array of ~12 Gaussian wave packets, initially spaced by $\lambda/2$ and having $1/e$ widths of $\lambda/6$. (In the experiment, we shut off the lattice field with a ~40-μs ramp to achieve a relatively large initial wave packet extent. This ensures that the interference profiles contain at most two peaks.) We account for squeezing by assigning a random phase to each wave packet, with this random phase being derived from a Gaussian distribution with a prescribed variance that is a function of the squeezing factor and the number of atoms in the lattice site. We then allow the wave packets to evolve for 8 ms (the same interval used in the experiment) and calculate the probability distribution associated with the resulting wave function. To compare this simulated distribution with experiment, we convolve it with a Gaussian resolution function, the width of which is inferred from our sharpest images. Finally, we fit the convolved waveform with the same fit function we apply to our data, to obtain a relation between the squeezing factor and ζ. We account for the stochastic nature of the simulation by repeating this procedure many times for a given set of parameters, to obtain an average ζ for a given squeezing factor.

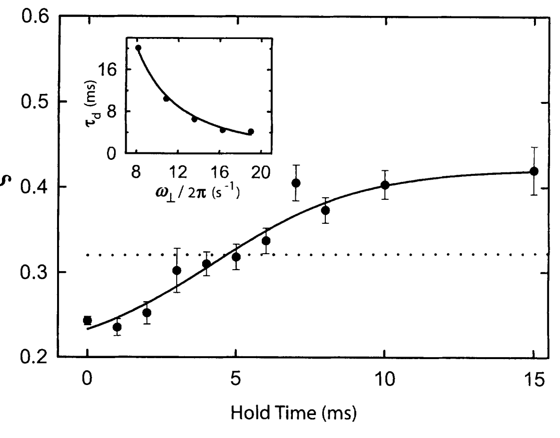

Fig. 3. Dephasing due to inhomogeneous phase broadening. The points show ζ as a function of hold time after loading into a lattice with $U_0 \sim 30\ E_R$, $\tau_r = 2$ ms, and $\omega_\perp = 2\pi \times 19\ \mathrm{s}^{-1}$. The solid line is a sigmoid fit to the data to extract a dephasing time. The dotted line shows the behavior of a lattice with $U_0 = 18\ E_R$ and $\tau_r = 200$ ms. **(Inset)** Dephasing time τ_d as a function of radial trap frequency $\omega_\perp$. The solid line shows a fit to $\omega_\perp^{-2}$ (the curvature of the harmonic TOP potential scales as $\omega_\perp^2$).

4A. In this case, we see no substantial difference between ζ after release from $U_0^{(\max)}$ and ζ measured after the slow reduction to $U_0^{(\mathrm{release})}$. This confirms that the reduction in phase variance seen in Fig. 4D represents an adiabatic transition from a coherent state to a squeezed state back to a coherent state and is not the result of a rephasing or recondensing of the system as the lattice potential is slowly lowered (*33*).

An estimate for the adiabaticity time scale is given by data for several different initial ramp speeds with the same 150-ms ramp down time (Fig. 5). We see a rapid increase in ζ between ramp times of 2 and 15 ms. For a $U_0^{(\max)} = 30\ E_R$ lattice, our data indicate a time scale for adiabaticity with respect to the many-body ground state of ~4 ms, consistent with the frequency of low-lying phonon excitations $\omega_m \simeq \sqrt{8Ng\beta\gamma}|\sin \pi m/n_l|$ (integer $|m| \leq n_l/2$, where n_l is the number of lattice sites) for our parameters (*20*).

The interferometric method used to measure the phase variance opens the exciting possibility of studying the dynamic evolution of the quantum state after a diabatic change in the lattice potential. If we prepare a number-squeezed state in the lattice, make a sudden change in the potential, and wait some time before releasing the atoms from the trap, we can stroboscopically follow the phase spread as a function of time and watch the squeezed state evolve in the new potential. Numerical simulations predict an oscillation between number-squeezed and phase-squeezed states in such a system, which should be readily visible using our interferometric phase probe. Future experiments will focus on the dynamic behavior of the system, with an eye toward the ultimate goal of Heisenberg-limited atom interferometry with squeezed states.

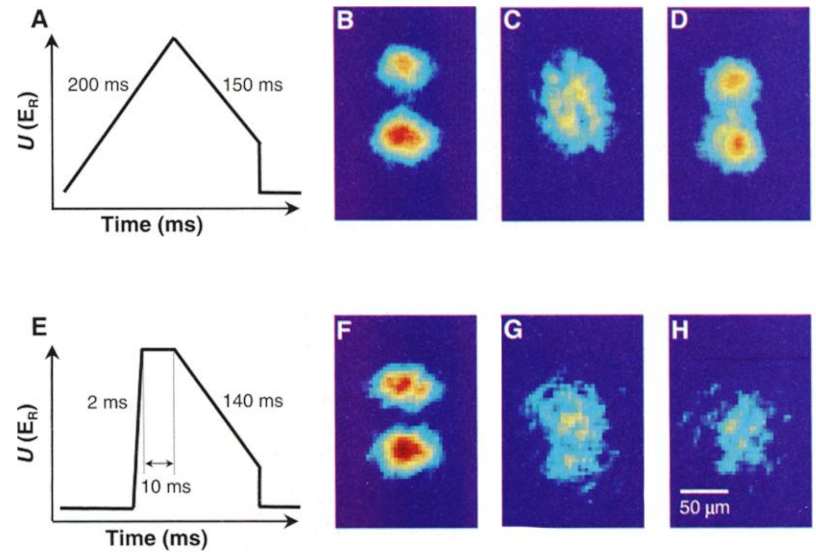

Fig. 4. Adiabatic transitions between squeezed and coherent states. (**A**) Schematic of the lattice intensity modulation used in the experiment. (**B**) Absorption image of atoms released from a lattice with $U_0 = 12\ E_R$. (**C**) Absorption image of atoms released from a lattice with $U_0 = 41\ E_R$. (**D**) Absorption image of atoms released after application of the intensity modulation shown in (A). (**E**) Schematic of the intensity ramp for $\tau_r = 2$ ms. Atoms are held at the maximum lattice depth for 10 ms to allow inhomogeneous dephasing. (**F**) Absorption image after release from a lattice with $U_0 = 12\ E_R$. (**G**) Absorption image of atoms released from a lattice with $U_0 = 36\ E_R$. (**H**) Absorption image of atoms released after application of the intensity ramp shown in (E).

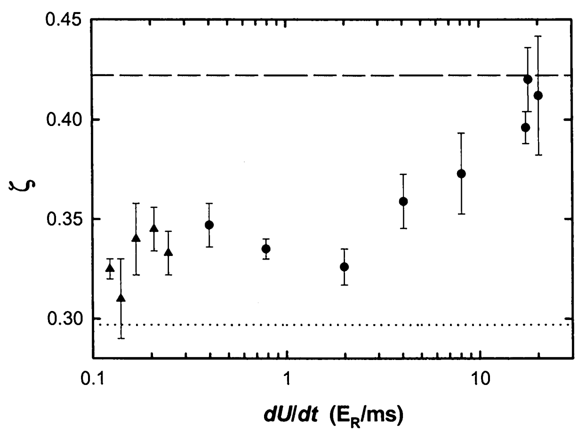

Fig. 5. ζ as a function of initial ramp speed $dU/dt = U_0^{(\max)}/\tau_r$. The lattice is increased to $U_0^{(\max)}$, held for 10 ms, and then reduced to $U_0^{(\mathrm{release})}$ over 140 ms. The dotted line represents the average contrast for atoms released from an 8 E_R lattice; the dashed line represents the average contrast for dephased samples. Circles represent points with $U_0^{(\max)} = 30\ E_R$ and different ramp times τ_r. Triangles represent points with $\tau_r = 200$ ms and different $U_0^{(\max)}$.

References and Notes

1. See, e.g., D. F. Walls, G. J. Milburn, *Quantum Optics* (Springer-Verlag, Berlin, 1994).
2. C. M. Caves, *Phys. Rev. D* **23**, 1693 (1981).
3. P. Berman Ed., *Atom Interferometry* (Academic Press, New York, 1997).
4. P. Bouyer, M. A. Kasevich, *Phys. Rev. A* **56**, R1083 (1997).
5. J. Hald, J. L. Sørensen, C. Schori, E. S. Polzik, *Phys. Rev. Lett.* **83**, 1319 (1999).
6. C. A. Sackett *et al.*, *Nature* **404**, 256 (2000).
7. A. Kuzmich, L. Mandel, N. P. Bigelow, *Phys. Rev. Lett.* **85**, 1594 (2000).
8. M. Kitagawa, M. Ueda, *Phys. Rev. A* **47**, 5138 (1993).
9. D. Wineland, J. Bollinger, W. Itano, F. Moore, D. Heinzen, *Phys. Rev. A* **46**, R6797 (1992).
10. R. W. Spekkens, J. E. Sipe, *Phys. Rev. A* **59**, 3868 (1999).
11. J. Javanainen, M. Yu. Ivanov, *Phys. Rev. A* **60**, 2351 (1999).
12. A. Imamoğlu, M. Lewenstein, L. You, *Phys. Rev. Lett.* **78**, 2511 (1997).
13. $\gamma \equiv \int d^3r\phi_l(r)\,[(-\hbar^2/2m\nabla^2 + U(r)]\phi_r(r)$ and $\beta \equiv \int d^3r\phi_l^2\phi_r^2$, where $\phi_{l,r}$ are the left- and right-well single-particle states and $U(r)$ is the external potential.
14. P. Horak, S. M. Barnett, *J. Phys. B Atom. Mol. Opt. Phys* **32**, 3421 (1999).
15. This result assumes repulsive interactions between atoms ($a_{sc} > 0$). In the case of a condensate with attractive interactions between atoms ($a_{sc} < 0$), the ground state is an N-particle Schrödinger cat state—a coherent superposition of states with all *N* atoms in the left or right well.
16. S. Sachdev, *Quantum Phase Transitions* (Cambridge Univ. Press, New York, 2000).
17. B. P. Anderson, M. A. Kasevich, *Science* **282**, 1686 (1998).
18. ———, in *Proceedings of the International School of Physics "Enrico Fermi," Course CXL*, M. Inguscio, S. Stringari, C. Wieman, Eds. (IOS Press, Amsterdam, 1999), pp. 439–452.
19. M. P. Fischer, P. B. Weichman, G. Grinstein, D. Fisher, *Phys. Rev. B* **40**, 546 (1989).
20. J. Javanainen, *Phys. Rev. A* **60**, 4902 (1999).
21. D. Jaksch, C. Bruder, J. I. Cirac, C. W. Gardiner, P. Zoller, *Phys. Rev. Lett.* **81**, 3108 (1998).
22. T. L. Ho, S. K. Yip, *Phys. Rev. Lett.* **84**, 4031 (2000).
23. H. Pu, S. Raghavan, N. P. Bigelow, *Phys. Rev. A* **61**, 023602 (2000).
24. B. P. Anderson, M. A. Kasevich, *Phys. Rev. A* **59**, R938 (1999).
25. D. S. Jin, J. R. Ensher, M. R. Matthews, C. E. Wieman, E. A. Cornell, *Phys. Rev. Lett.* **77**, 420 (1996).
26. M. O. Mewes *et al.*, *Phys. Rev. Lett.* **77**, 988 (1996).
27. The rotating magnetic field component of the TOP (in the plane perpendicular to the lattice) is left on to maintain the orientation of the atoms in the sample.
28. The phase difference between neighboring wells due to the gravitational potential is $\Delta\phi = (mg\lambda/2\hbar)t_h$, where t_h is the hold time. See (*17*).
29. Y. Castin, J. Dalibard, *Phys. Rev. A* **55**, 4330 (1997).
30. J. Javanainen, S. M. Yoo, *Phys. Rev. Lett.* **76**, 161 (1996).
31. G. Baym, C. J. Pethick, *Phys. Rev. Lett.* **76**, 6 (1996).
32. Another possible dephasing mechanism would be the coherent state self-dephasing discussed in (*12*). Theoretical estimates suggest a time scale for this process on the order of 100 ms.
33. Numerical integration of the equations of motion for an array of coherent states with random phases confirms that no rephasing of the wave functions is expected during the lowering of the lattice potential.

34. This work was supported by the NSF, the Army Research Office, and the Office of Naval Research. We thank W. Ketterle, S. Sachdev, and J. Sipe for useful discussions.

11 December 2000; accepted 16 February 2001